

Impurity States in Transition Metals

A. M. CLOGSTON

Bell Telephone Laboratories, Murray Hill, New Jersey

(Received 23 June 1964)

The Green's-function technique of Slater and Koster is used to formulate the Hartree-Fock problem for impurities in transition metals. Partial account is taken of the many-band structure of the transition metals and of electron-electron correlation. Application is made to the solution of the self-consistent-field equations in simple cases, to a generalized condition for magnetization of an impurity, to polarization of near-neighbor atoms, to the Knight shift of impurity atoms, and to the occurrence of a magnetic moment as a function of electron concentration for Fe dissolved in the bcc 4*d* transition metals. It is concluded that the effective exchange energies that act to magnetize transition-metal impurities are no greater than 1–2 eV.

I. INTRODUCTION

THE electronic structure of widely separated impurities in transition metals has received increasing attention in recent years. This interest is in response to expanding experimental measurements of susceptibility, specific heat, conductivity, nuclear magnetic resonance, Mössbauer effect, and neutron diffraction. Some theoretical progress has been made in the analysis of these observations, but the work is still in an early stage. This is not surprising since a real understanding of the electronic structure of the pure transition metals is just beginning to emerge. Work by Friedel,¹ Kohn and Vosko,² and many others³ has established some of the basic ideas concerning the electronic structure of impurities in metals, but these efforts have been most appropriately applied to the study of *s-p* band metals and to the asymptotic behavior of wave functions around an impurity. More recent work by Anderson,⁴ Wolf,⁵ and Clogston^{6,7} has applied methods better suited to the narrow bands encountered in *d*-band and *f*-band metals. In particular, the Green's function method introduced by Slater and Koster^{8–10} has been developed and applied in a preliminary way to various impurity problems, including the interesting question of magnetized local states.^{4–6}

In its simplest form, the Green's function method has been used by Wolff⁵ to determine the wave functions of a single band of electrons in the presence of an impurity atom under the assumption that the impurity potential is closely confined to the site of the foreign atom. These wave functions are then used to determine the self-consistent Hartree-Fock potential for the impurity. The

method has been applied principally to discussing the conditions under which an isolated impurity atom will magnetize when dissolved in a transition metal solute. In this paper we want to extend the discussion and make it more realistic by taking partial account of correlation and the many-band structure of the transition metals. We can then give a fuller account of the electronic events that occur around an impurity atom. We shall also give a more general account of the conditions under which an impurity will magnetize, a calculation of the Knight shift of an impurity atom showing how it can depart widely from simple theory, and a semiquantitative discussion of the magnetic moment associated with an iron atom dissolved in the body-centered-cubic 4*d* transition metals.

II. THEORY

a. Exact Hartree-Fock Theory

The major results of the Green's function method can be recapitulated as follows.^{8–10} If E_{nk}^0 are the unperturbed eigenvalues for some pure metal, the perturbed wave functions for energy $E = E_{nk}^0$ and spin σ are expanded in terms of the Wannier functions $W_n(\mathbf{r} - \mathbf{r}_a) \equiv W_{na}(\mathbf{r})$ for band n and site a .

$$\Psi_{nk\sigma}(\mathbf{r}) = \frac{1}{\sqrt{N}} \sum_{ma} A_{m\sigma}(\mathbf{r}_a) W_{ma}(\mathbf{r}), \quad (1)$$

where N is the number of atoms in the crystal. Then $A_{m\sigma}(\mathbf{r}_a)$ is given by

$$A_{m\sigma}(\mathbf{r}_a) = \delta_{nm} e^{i\mathbf{k} \cdot \mathbf{r}_a} + \sum_b G_{mE}(\mathbf{r}_a - \mathbf{r}_b) c_{m\sigma}(\mathbf{r}_b), \quad (2)$$

where

$$G_{nE}(\mathbf{r}) = \frac{1}{N} \sum_{\mathbf{k}} \frac{e^{i\mathbf{k} \cdot \mathbf{r}}}{E_{n\mathbf{k}}^0 - E} \quad (3)$$

and the $c_{m\sigma}(\mathbf{r}_b)$ satisfy the difference equations

$$c_{m\sigma}(\mathbf{r}_b) + \sum_{lc} (W_{mb} | V_{\sigma}^{\text{HF}} | W_{lc}) \times [\delta_{nl} e^{i\mathbf{k} \cdot \mathbf{r}_c} + \sum_d G_{lE}(\mathbf{r}_c - \mathbf{r}_d) c_{l\sigma}(\mathbf{r}_d)] = 0. \quad (4)$$

V_{σ}^{HF} is the self-consistent Hartree-Fock potential for

¹ P. F. Casteljan and J. Friedel, *J. Phys. Radium* **17**, 27 (1956); *J. Friedel, Can. J. Phys.* **39**, 1190 (1956); *J. Phys. Radium* **19**, 573 (1958); *Nuovo Cimento Suppl.* **2** **7**, 287 (1958). These papers contain extensive bibliographies to early work.

² W. Kohn and S. H. Vosko, *Phys. Rev.* **119**, 912 (1960).

³ Summaries of recent work and many references may be found in the volume *Metallic Solid Solutions*, edited by J. Friedel and A. Guinier (W. A. Benjamin, Inc., New York, 1963).

⁴ P. W. Anderson, *Phys. Rev.* **124**, 41 (1961).

⁵ P. A. Wolff, *Phys. Rev.* **124**, 1030 (1961).

⁶ A. M. Clogston, B. T. Matthias, M. Peter, H. J. Williams, E. Corenzwit, and R. C. Sherwood, *Phys. Rev.* **125**, 541 (1962).

⁷ A. M. Clogston, *Phys. Rev.* **125**, 439 (1962).

⁸ G. F. Koster and J. C. Slater, *Phys. Rev.* **95**, 1167 (1954).

⁹ G. F. Koster, *Phys. Rev.* **95**, 1436 (1954).

¹⁰ G. F. Koster and J. C. Slater, *Phys. Rev.* **96**, 1208 (1954).

spin σ and is given by

$$\begin{aligned} & (W_{na} | V_{\sigma}^{\text{HF}} | W_{mb}) \\ &= (W_{na} | -Ze^2/r | W_{mb}) \\ &+ \sum_{lk\sigma'} [(\Psi_{lk\sigma'} W_{na} | e^2/r_{12} | \Psi_{lk\sigma'} W_{mb}) \\ &- (\Psi_{lk^0} W_{na} | e^2/r_{12} | \Psi_{lk^0} W_{mb})] \\ &- \sum_{lk} [(\Psi_{lk\sigma} W_{na} | e^2/r_{12} | W_{mb} \Psi_{lk\sigma}) \\ &- (\Psi_{lk^0} W_{na} | e^2/r_{12} | W_{mb} \Psi_{lk^0})]. \quad (5) \end{aligned}$$

The direct potential due to the impurity nucleus is $-Ze^2/r$, and the unperturbed wave functions are Ψ_{nk^0} . The summations on k extend over filled states up to the Fermi level. In principle, the systems of Eqs. (4) and (5) can be solved simultaneously giving a complete solution of the impurity problem within the Hartree-Fock approximation.

b. Approximate Hartree-Fock Theory

In order to get a manageable theory, we must introduce some drastic assumptions. We suppose, therefore, that the impurity potential is large only near the impurity site $r_0=0$, and that only diagonal elements of V_{σ}^{HF} exist between the various bands. These are essentially the same assumptions made by Wolff,⁵ except that we consider several bands to be important in screening the impurity. We thus retain in an approximate way some important features of the many-band structure, as is seen below. We have, then,

$$c_{m\sigma}(0) = -\delta_{nm} \frac{(W_{m0} | V_{\sigma}^{\text{HF}} | W_{m0})}{1 + (W_{m0} | V_{\sigma}^{\text{HF}} | W_{m0}) G_{mE}(0)} \quad (6)$$

and

$$A_{m\sigma}(r_a) = \delta_{nm} \left[e^{ik \cdot r_a} - \frac{(W_{m0} | V_{\sigma}^{\text{HF}} | W_{m0}) G_{mE}(r_a)}{1 + (W_{m0} | V_{\sigma}^{\text{HF}} | W_{m0}) G_{mE}(0)} \right]. \quad (7)$$

We next rewrite Eq. (1) as

$$\Psi_{nk\sigma}(r) = (1/\sqrt{N}) [A_{n\sigma}(0) W_{n0}(r) + \sum_{a \neq 0} A_{n\sigma}(r_a) W_{na}(r)] \quad (8)$$

and define $V_{n\sigma} \equiv (W_{n0} | V_{\sigma}^{\text{HF}} | W_{n0})$ so that

$$\Psi_{nk\sigma} = \frac{1}{\sqrt{N}} \left[\frac{1}{1 + V_{n\sigma} G_{nE}(0)} W_{n0}(r) + \sum_{a \neq 0} A_{n\sigma}(r_a) W_{na}(r) \right]. \quad (9)$$

We now further approximate by using in Eq. (5) only that part of $\Psi_{lk\sigma}$ depending on $W_{l0}(r)$. Equation (5)

then becomes

$$\begin{aligned} V_{n\sigma} &= (W_{n0} | -Ze^2/r | W_{n0}) \\ &+ \frac{1}{N} \sum_{lE\sigma'} \left[(W_{l0} W_{n0} | e^2/r_{12} | W_{l0} W_{n0}) \right. \\ &- \delta_{\sigma\sigma'} \left(W_{l0} W_{n0} \left| \frac{e^2}{r_{12}} \right| W_{n0} W_{l0} \right) \left. \right] \\ &\times \left[\frac{1}{1 + V_{l\sigma'} G_{lE}(0)} - 1 \right]. \quad (10) \end{aligned}$$

The Green's function $G_{nE}(0)$ may be written

$$G_{nE}(0) = \int \frac{\eta_n(E') dE'}{E' - E}, \quad (11)$$

where $\eta_n(E)$ is the density of states per atom in the unperturbed band n and the integral is extended over the whole band. The principal part of this integral is set equal to $-I_n(E)$ so that

$$G_{nE}(0) = -I_n(E) + i\pi\eta_n(E). \quad (12)$$

A discussion of the functional form of $I_n(E)$ is given in Ref. 7. Equation (10) is now written

$$\begin{aligned} V_{n\sigma} &= (W_{n0} | -Ze^2/r | W_{n0}) \\ &+ \sum_{l\sigma'} [(W_{l0} W_{n0} | e^2/r_{12} | W_{l0} W_{n0}) \\ &- \delta_{\sigma\sigma'} (W_{l0} W_{n0} | e^2/r_{12} | W_{n0} W_{l0})] \\ &\times \int \eta_l(E) \left[\frac{1/V_{l\sigma'}^2}{(I_l - 1/V_{l\sigma'})^2 + (\pi\eta_l)^2} - 1 \right] dE. \quad (13) \end{aligned}$$

The integral in Eq. (13) is the number of electrons $N_{l\sigma}$ of spin σ accumulated on the impurity site by the perturbation from band l .

We next further simplify Eq. (13) by assuming that all the Coulomb integrals are equal to U , the exchange integrals between identical Wannier functions are equal to J , and the exchange integrals between different Wannier functions are equal to K . Setting $(W_{n0} | -Ze^2/r | W_{n0}) = -ZF$, we have

$$\begin{aligned} V_{n\sigma} &= -ZF + \sum_{\sigma'} (U - \delta_{\sigma\sigma'} J) N_{n\sigma'} \\ &+ \sum_{m \neq n, \sigma'} (U - \delta_{\sigma\sigma'} K) N_{m\sigma'}. \quad (14) \end{aligned}$$

We suppose specifically that J is much smaller than U . This assumption is contrary to previous work,⁴⁻⁶ in which J has been taken equal to U . It seems evident, however, that J must be greatly reduced by correlation. For an iron atom in the configuration d^8 , F is about 30

eV and U is about 20 eV,¹¹ while we present evidence below that J cannot be larger than 1–2 eV. The exchange integral K will probably be smaller than the exchange integral between orthogonal orbits in Fe, which is about 0.6 eV, and therefore is probably in the range 0.1 to 0.5 eV. It also becomes evident below that U cannot be greatly reduced below its free-atom value without changing the nature of the impurity problem in a way contrary to the general experimental evidence. It is to be expected that correlation should have a much larger effect upon the exchange integrals than upon the Coulomb integrals. A discussion of this important point has been given by Phillips¹² in connection with the effect of correlation on the self-consistent field problem of a pure metal.

c. Approximation for $N_{n\sigma}$

The total charge of spin σ in states brought below the Fermi level by the perturbation is given by $1/\pi$ times the phase shift $\gamma_{n\sigma}(E_f)$ of electrons at the Fermi surface.⁷ The phase shift is given by

$$\gamma_{n\sigma}(E_f) = \tan^{-1} \frac{\pi\eta_n(E_f)}{I_n(E_f) - 1/V_{n\sigma}}. \quad (15)$$

For most simple band shapes $(1/\pi)\gamma_{n\sigma}(E_f)$ is a good approximation to $N_{n\sigma}$. The two quantities are exactly equal for a Lorentzian density of states and very similar in other cases. In order to avoid discussing specific band shapes in what follows, we approximate by taking $N_{n\sigma} = (1/\pi)\gamma_{n\sigma}(E_f)$. If we set $\alpha_n = I_n(E_f)/\pi\eta_n(E_f)$, we have therefore

$$N_{n\sigma} = (1/\pi) \tan^{-1} \left\{ \left[\alpha_n - \frac{1}{\pi\eta_n(E_f)V_{n\sigma}} \right]^{-1} \right\}. \quad (16)$$

In Fig. 1 we present a set of curves giving $N_{n\sigma}$ as a function of $\pi\eta_n(E_f)V_{n\sigma}$ for various values of α_n . The curves are drawn for $V_{n\sigma}$ negative. A set of curves for $V_{n\sigma}$ positive can be obtained by reversing the signs of $V_{n\sigma}$, α_n and $N_{n\sigma}$. For $V_{n\sigma}$ very large, $N_{n\sigma}$ saturates at a value $\pi^{-1} \tan^{-1}(1/\alpha_n)$. This is a measure of how many states per atom lie above the Fermi level. Thus large positive values of α correspond to a nearly filled band, and large negative values of α to a nearly empty band. The impurity cannot ever depress below the Fermi level more states per band than were available in the unperturbed band above the Fermi level. For $V_{n\sigma}$ small, $N_{n\sigma} = -\eta_n(E_f)V_{n\sigma}$, which is just the Thomas-Fermi assumption.

d. Perturbation of Nearest Neighbors

We see below that an impurity will not usually be completely screened on the impurity site. In that case a

¹¹ R. E. Watson, Technical Report No. 12, Solid State and Molecular Theory Group—MIT, Cambridge, Massachusetts, 1959 (unpublished) and Phys. Rev. **118**, 1036 (1960).

¹² J. C. Phillips, Phys. Rev. **123**, 420 (1961).

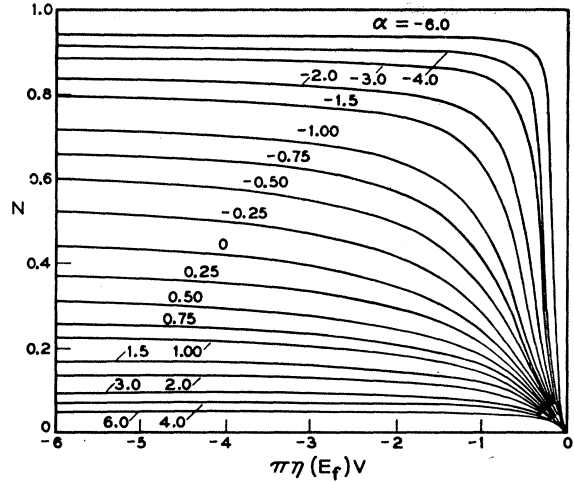


FIG. 1. A plot of $N = 1/\pi \tan^{-1}[\alpha - 1/\pi\eta(E_f)V]^{-1}$ as a function of $\pi\eta(E_f)V$ for various values of α . For positive values of $\pi\eta(E_f)V$, reverse the sign of N and α .

perturbation extends to the nearest-neighbor site, and a subsidiary self-consistent potential problem will exist. Returning to Eq. (5), we may write for the direct potential at a neighboring site (a), due to the self-consistent potential established at $r=0$,

$$\begin{aligned} (W_{na} | V_{\sigma}^{\text{HF}} | W_{na}) &= (W_{na} | -Ze^2/r | W_{na}) \\ &+ \sum_{lk\sigma'} [(\Psi_{lk\sigma'} W_{na} | e^2/r_{12} | \Psi_{lk\sigma'} W_{na}) \\ &- (\Psi_{lk^0} W_{na} | e^2/r_{12} | \Psi_{lk^0} W_{na})] \\ &- \sum_{lk} [(\Psi_{lk\sigma} W_{na} | e^2/r_{12} | W_{na} \Psi_{lk\sigma}) \\ &- (\Psi_{lk^0} W_{na} | e^2/r_{12} | W_{na} \Psi_{lk^0})]. \quad (17) \end{aligned}$$

We approximate once again by replacing $\Psi_{lk\sigma}$ by the first term of Eq. (9) and then obtain

$$\begin{aligned} (W_{na} | V_{\sigma}^{\text{HF}} | W_{na}) &= (W_{na} | -Ze^2/r | W_{na}) \\ &+ \sum_{l\sigma'} [(W_{l0} W_{na} | e^2/r_{12} | W_{l0} W_{na}) \\ &- \delta_{\sigma\sigma'} (W_{l0} W_{na} | e^2/r_{12} | W_{na} W_{l0})] N_{l\sigma'}. \quad (18) \end{aligned}$$

This equation can be written approximately as

$$(W_{na} | V_{\uparrow}^{\text{HF}} | W_{na}) = (e^2/R)(-Z + N_{\uparrow} + N_{\downarrow}) - jN_{\uparrow}, \quad (19)$$

where R is the distance to site a , $N_{\sigma} = \sum_n N_{n\sigma}$, and we have set $(W_{l0} W_{na} | e^2/r_{12} | W_{na} W_{l0}) = j$ for all l and n .

Let us define the direct potential at the nearest-neighbor site $v_{\sigma} \equiv (W_{na} | V_{\sigma}^{\text{HF}} | W_{na})$, so that

$$v_{\uparrow} = (e^2/R)(-Z + N_{\uparrow} + N_{\downarrow}) - jN_{\uparrow}. \quad (20)$$

Usually, v_σ will be small enough so that one can write for the nearest-neighbor site from Eqs. (14) and (16),

$$N_{n\sigma'} = -\eta_n(E_f)V_{n\sigma'} \quad (21)$$

$$V_{n\sigma'} = v_\sigma + \sum_{\sigma'm} (U' - \delta_{\sigma\sigma'}J')N_{m\sigma'}, \quad (22)$$

where we have taken $K'=J'$ for simplicity. These equations may be solved simultaneously to give

$$\sum_m (N_{m\uparrow'} + N_{m\downarrow'}) = -\frac{v_\uparrow + v_\downarrow}{1 + (2U' - J')\xi(E_f)} \xi(E_f), \quad (23)$$

$$\sum_m (N_{m\uparrow'} - N_{m\downarrow'}) = -\frac{(v_\uparrow - v_\downarrow)}{1 - \xi(E_f)J'} \xi(E_f). \quad (24)$$

Here the primes denote quantities appropriate for the neighbor, or regular, lattice site, and $\xi(E_f)$ is the total density of states for all bands defined by $\xi(E_f) = \sum_n \eta_n(E_f)$. Equations (23) and (24) are used below in discussing the distribution of shielding charge over the nearest-neighbor atoms to an impurity and in considering the polarization of neighbor atoms to a magnetic impurity.

In this discussion of the nearest-neighbor atoms, we have presumed that each neighbor atom is acting independently of all other neighbors. Actually this is not so. Complicated interference effects exist between the wave

functions at the various neighbor sites that have been discussed by Slater and Koster.¹⁰ These effects are usually rather small and are neglected for simplicity.

e. One Dominant Band

It may happen in an impurity problem that the burden of shielding the impurity rests largely upon one dominant band. This is the case if all other bands present a low density of states at the Fermi level by reason of being nearly or completely filled or empty. In this case, let us take $n=1$ to be the dominant band and $n=l, m, \dots$ to be the remaining bands. We suppose $\eta_l(E_f)$ to be small enough so that $N_{l\sigma} = -\eta_l(E_f)V_{l\sigma}$. Then Eq. (14) may be written

$$V_{1\sigma} = -ZF + \sum_{\sigma'} (U - \delta_{\sigma\sigma'}J)N_{1\sigma'} - \sum_{l\sigma'} (U - \delta_{\sigma\sigma'}K)\eta_l(E_f)V_{l\sigma'}, \quad (25)$$

$$V_{l\sigma} = -ZF - \sum_{\sigma'} (U - \delta_{\sigma\sigma'}J)\eta_l(E_f)V_{l\sigma'} + \sum_{\sigma'} (U - \delta_{\sigma\sigma'}K)N_{1\sigma'} - \sum_{m \neq l\sigma'} (U - \delta_{\sigma\sigma'}K)\eta_m(E_f)V_{m\sigma'}. \quad (26)$$

These two equations can be solved simultaneously, with the results

$$\left. \begin{aligned} \frac{1}{2}(V_{1\uparrow} + V_{1\downarrow}) &= -\frac{ZF}{1 + (2U - K)\beta} + \frac{2U - J}{1 + (2U - K)\beta} \left[1 + \frac{2U - K}{2U - J}(K - J)\beta \right] \frac{1}{2}(N_{1\uparrow} + N_{1\downarrow}) \\ (V_{1\uparrow} - V_{1\downarrow}) &= -\frac{J}{1 - K\beta} \left[1 + \frac{K}{J}(K - J)\beta \right] (N_{1\uparrow} - N_{1\downarrow}) \end{aligned} \right\}, \quad (27)$$

$$\left. \begin{aligned} \frac{1}{2}(N_{1\uparrow} + N_{1\downarrow}) &= -\frac{\eta_l(E_f)}{[1 - (J - K)\eta_l][1 + (2U - K)\beta]} [-ZF + (2U - K)\frac{1}{2}(N_{1\uparrow} + N_{1\downarrow})] \\ (N_{1\uparrow} - N_{1\downarrow}) &= \frac{K\eta_l(E_f)}{[1 - (J - K)\eta_l][1 - K\beta]} (N_{1\uparrow} - N_{1\downarrow}) \end{aligned} \right\}, \quad (28)$$

where

$$\beta = \sum_l \frac{\eta_l(E_f)}{1 - (J - K)\eta_l(E_f)}. \quad (29)$$

If, for simplicity, we again place $K=J$, the four equations can be put in the form

$$\left. \begin{aligned} \frac{1}{2}(V_{1\uparrow} + V_{1\downarrow}) &= \{1/[1 + (2U - J)\beta]\} [-ZF + (2U - J)\frac{1}{2}(N_{1\uparrow} + N_{1\downarrow})] \\ (V_{1\uparrow} - V_{1\downarrow}) &= -[J/(1 - J\beta)](N_{1\uparrow} - N_{1\downarrow}) \end{aligned} \right\}, \quad (30)$$

$$\left. \begin{aligned} \frac{1}{2}(N_{1\uparrow} + N_{1\downarrow}) &= -\{\eta_l(E_f)/[1 + (2U - J)\beta]\} [-ZF + (2U - J)\frac{1}{2}(N_{1\uparrow} + N_{1\downarrow})] \\ (N_{1\uparrow} - N_{1\downarrow}) &= [J\eta_l(E_f)/(1 - J\beta)](N_{1\uparrow} - N_{1\downarrow}) \end{aligned} \right\}, \quad (31)$$

where now $\beta = \sum_l \eta_l(E_f)$. If we place $\beta=0$ in Eq. (30), we obtain the appropriate relations for a single band, as would be found directly from Eq. (14). It is clear that the effect of the other bands is to shield the potentials

$-ZF$ and $(2U - J)$ experienced by band 1. The magnetic effects, however, which, we see below, derive from the second of Eqs. (30) are enhanced by the presence of the other bands.

It should be remarked here that this analysis remains approximately correct even if one of the low-state density subsidiary bands has the character of a wide s band. In that case, the Fourier transform of the self-consistent charge density of one spin is

$$\rho(q) = V(q)F(q), \quad (32)$$

where $V(q)$ is the Fourier transform of the self-consistent potential. $F(q)$ is given by

$$F(q) = -\frac{1}{v} \sum_k \frac{n_{k+q} - n_k}{E_{k+q} - E_k}, \quad (33)$$

where v is the volume of the system and n_k is the occupation number of state E_k . One has

$$\lim_{q \rightarrow 0} F(q) = - (1/\Omega) \eta(E_f),$$

where $\eta(E_f)$ is the s -band density of states per atom and Ω is the atomic volume. The total charge accumulated from the s band is then

$$v\rho(0) = - (v/\Omega) V(0) \eta(E_f). \quad (34)$$

Since the self-consistent potential including contributions from the s band will be closely confined to the impurity site, $(v/\Omega) V(0)$ will be approximately the same as the self-consistent potential experienced by the d -bands, so that Eq. (34) is consistent with the assumptions made earlier in this section.

III. APPLICATIONS

a. Some Simple Examples

In this section, we consider a simple case of an impurity problem to illustrate the range of electronic events that may occur around an impurity. We consider first a single band of electrons and a nonmagnetic case in which $N_\uparrow = N_\downarrow = N$ and $V_\uparrow = V_\downarrow = V$. Equations (14) and (16) then become

$$V = -ZF + (2U - J)N, \quad (35)$$

$$N = (1/\pi) \tan^{-1} \left\{ \left[\alpha - \frac{1}{\pi\eta(E_f)V} \right]^{-1} \right\}. \quad (36)$$

These two equations must be solved simultaneously to find V and N . As an example, we take the valence contrast of the impurity $Z=1$ and adopt the values $F=30$ eV, $U=20$ eV, and $J=2$ eV. We furthermore consider a Lorentzian band for which

$$\eta(E) = \frac{1}{\pi\Delta} \frac{1}{1 + (E/\Delta)^2}, \quad (37)$$

$$I(E) = \frac{1}{\Delta} \frac{(E/\Delta)}{1 + (E/\Delta)^2}, \quad (38)$$

$$\alpha = (E_f/\Delta), \quad (39)$$

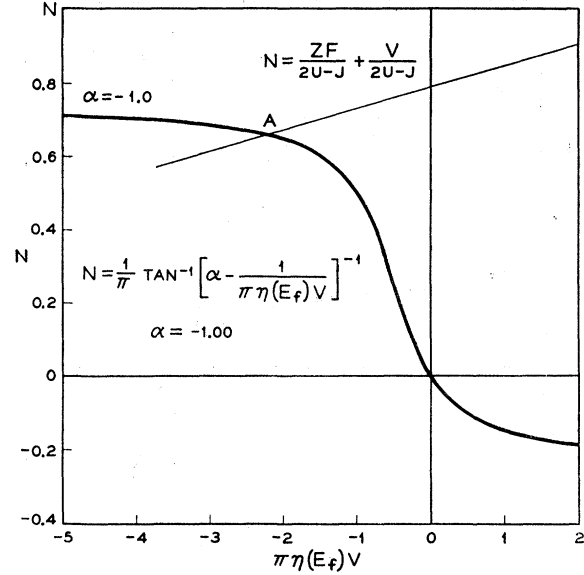


FIG. 2. Solution of Eqs. (35) and (36) in text for $F=30$, $U=20$, $J=2$, $Z=1$, $\alpha=-1$, and $\pi\eta(E_f)=0.5$.

so that $\Delta = 1/[\pi\eta(E_f)(1+\alpha^2)]$. Suppose we chose $\pi\eta(E_f)=0.5$ states/eV-atom, a value typical of $4d$ -band metals, and $\alpha=-1$. Then the band has a width of 1 eV and is $\frac{1}{4}$ filled. In Fig. 2, we show a curve for N as a function of $\pi\eta(E_f)V$ for $\alpha=-1$. Equation (35) is also shown as a straight line of slope $1/[\pi\eta(E_f)(2U-J)]$, intersecting the axis of ordinates at $ZF/(2U-J)$. The self-consistent potential determined by the intersection of the two curves at point A is -4.5 eV, contrasted with the direct impurity potential $-ZF=-30$ eV. The number of electrons accumulated around the impurity is $2N=1.32$, contrasted with the number $Z=1$ needed to just shield the impurity completely.

If exchange effects were ignored ($J=0$), if a localized electron were perfectly effective in shielding the nucleus ($U=F$), and if the density of states were very large, then $2N$ would be very nearly 1. This is evident since, then, Eq. (35) would define a straight line of very small slope intersecting the axis of ordinates at $Z/2$. In actual fact, as this example shows, because of exchange and imperfect shielding, there is a tendency for an excess of electrons to accumulate around a positive valence impurity. Both of these effects are absent from theories based on Poisson's equation and the Thomas-Fermi approximation or the Born approximation. This excess charge must be compensated by a spreading out of the perturbation to atoms adjacent to the impurity, which we discuss below. If J were not greatly reduced by correlation, or if U were equally reduced, the tendency of the perturbation to affect sites at a distance from the impurity atom would be exaggerated. This is contrary to the general experimental evidence that impurities in d -band metals are shielded almost entirely at the impurity site.

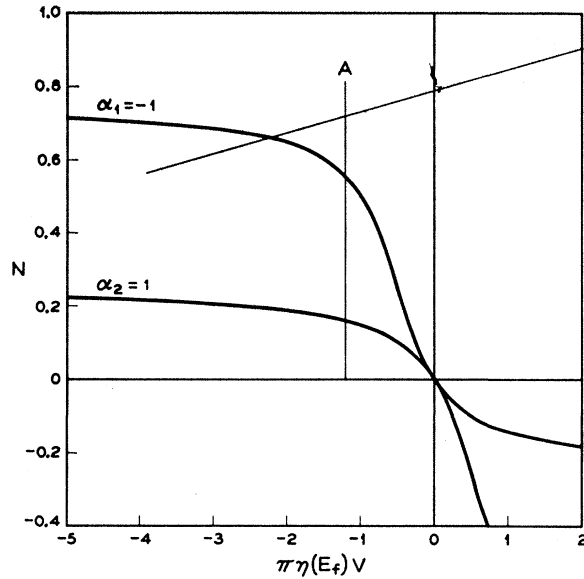


FIG. 3. Solution for the self-consistent potential for two bands with $\alpha_1 = -1$, $\pi\eta_1(E_f) = 0.5$, $\alpha_2 = 1$, $\pi\eta_2(E_f) = 0.5$, and other parameters as in Fig. 2.

Let us consider next in what way the above results would be affected by the presence of another band. For simplicity, we choose the second band to have the same density of states $\pi\eta(E_f) = 0.5$ but to have $\alpha = 1$. This band then also has a width of 1 eV but is $\frac{3}{4}$ filled. If we chose $K = J$ again for convenience, and name the two bands 1 and 2, it is clear from Eq. (14) that

$$V_1 = V_2 = -ZF + (2U - J)(N_1 + N_2). \quad (40)$$

Since we have chosen $\pi\eta(E_f)$ to be the same for both bands, we can find N_1 and N_2 from the construction shown in Fig. 3, where the self-consistent potential is marked by the line A and is chosen so that N_1 and N_2 add up to the value of N for which line A intersects Eq. (40). We now have $2N_1 = 1.12$ electrons and $2N_2 = 0.32$ electron for a total accumulation of 1.44 electrons, a somewhat larger number than resulted from the presence of only one band.

Finally, let us examine how the excess charge at the impurity site will affect its neighbors. With reference to Eq. (20), we suppose $R = 2 \text{ \AA}$ and neglect the small interatomic exchange effect by placing $j = 0$. If a_0 is the Bohr radius, \hbar^2/mc^2 equal to 0.529 \AA , $e^2/a_0 = 27.2 \text{ eV}$. Therefore, the direct potential at the nearest-neighbor site is $v = (27.2)(0.529/2)(0.44) = 3.15 \text{ eV}$. We have $\pi\xi(E_f) = 1.0 \text{ states/eV atom}$, and find then from Eq. (23) that there is an accumulation of 0.15 holes on each neighbor. These holes react back on the central atom but have a small effect in comparison to the original perturbation of 30 eV. In this approximate sense, the behavior of the complex is consistent with the original assumption that the perturbation is small except at the impurity site. The self-consistent potential at each near-

neighbor site is 0.48 eV and is much smaller at the next-nearest-neighbor site. Since we are using the Thomas-Fermi assumption $N = -\eta(E_f)V$, it is clear that the perturbation decreases essentially exponentially away from the impurity site with the characteristic Thomas-Fermi shielding constant

$$[8\pi e^2 \sum_n \eta_n(E_f)]^{1/2}.$$

b. Condition for Magnetization

In this section, we discuss the conditions under which an impurity in a metal will magnetize. We begin again with a single band. Equation (14) can then be written in the form

$$\frac{1}{2}(V_{\uparrow} + V_{\downarrow}) = -ZF + (2U - J)\frac{1}{2}(N_{\uparrow} + N_{\downarrow}), \quad (41)$$

$$(V_{\uparrow} - V_{\downarrow}) = -J(N_{\uparrow} - N_{\downarrow}). \quad (42)$$

These equations must now be solved simultaneously with Eq. (16) to find V_{\uparrow} , V_{\downarrow} , N_{\uparrow} , and N_{\downarrow} . It is clear from Eqs. (41) and (42) that these solutions can be found from the following construction. N as a function of $\pi\eta(E_f)V$ is first plotted from Eq. (16). Next draw a straight line on the plot with slope $-1/\pi\eta(E_f)J$. If this line intersects the curve at two points $(N_{\uparrow}, V_{\uparrow})$ and $(N_{\downarrow}, V_{\downarrow})$, these values satisfy Eq. (42). Next displace the straight line until the average of the two points $[1/2(N_{\uparrow} + N_{\downarrow}), 1/2(V_{\uparrow} + V_{\downarrow})]$ lies on the straight line going through the axis of ordinates at $ZF/(2U - J)$ with slope $1/[\pi\eta(E_f)(2U - J)]$. The two intersections then satisfy both Eqs. (41) and (42). An example is shown in Fig. 4. Here we have chosen $\pi\eta(E_f) = 3$, $Z = \frac{1}{2}$,

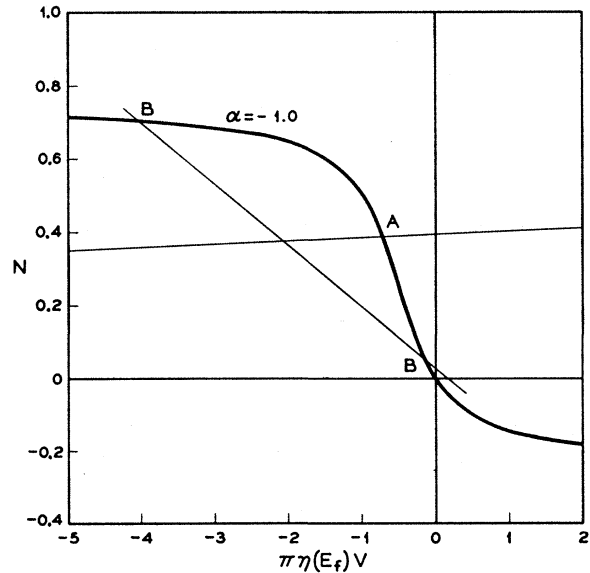


FIG. 4. Solution of the self-consistent problem in a case giving stable magnetic solutions at B and an unstable, nonmagnetic solution at A. Drawn for $F = 30$, $U = 20$, $J = 2$, $\alpha = -1$, $Z = \frac{1}{2}$, $\pi\eta(E_f) = 3$. See text for details of construction.

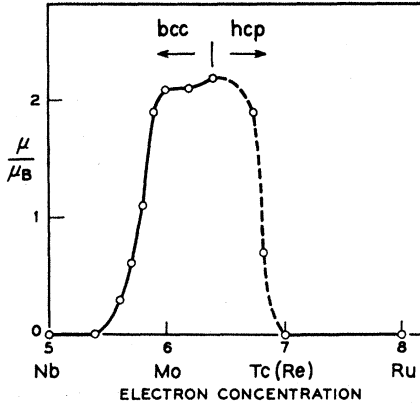


FIG. 5. Magnetic moment as a function of electron concentration for 1% of Fe in various 4d transition metal alloys from Ref. 6.

$\alpha = -1$, $F = 30$ eV, $U = 20$ eV, and $J = 2$ eV. The unstable nonmagnetic solution is shown at A, while the stable magnetic solutions are at the points marked B. The unstable solution corresponds to $2N = 0.78$ electron. The magnetic solution gives $(N_{\uparrow} + N_{\downarrow}) = 0.75$ electron and $(N_{\uparrow} - N_{\downarrow}) = 0.65$ Bohr magneton. It is obvious from the construction that the condition for a magnetic solution to exist is that

$$-dN/d(\pi\eta(E_f)V) > 1/\pi\eta(E_f)J \quad (43)$$

or simply

$$-dN/dV > 1/J. \quad (44)$$

From Eq. (16), we have

$$-\pi dN/d(\pi\eta(E_f)V) = \{[\alpha(\pi\eta(E_f)V) - 1]^2 + (\pi\eta(E_f)V)^2\}^{-1}, \quad (45)$$

so that the condition for instability can also be written

$$\eta(E_f)J > [\alpha(\pi\eta(E_f)V) - 1]^2 + (\pi\eta(E_f)V)^2. \quad (46)$$

This is a more general form of the condition found by Anderson⁴ and Wolf⁵ and reduces to their condition when a sharply defined local state exists. The right-hand side of condition (46) has a minimum value of $1/(1+\alpha^2)$ for $(\pi\eta(E_f)V) = \alpha/(\alpha^2+1)$, corresponding to a maximum value at this point of $dN/d(\pi\eta(E_f)V)$, equal to $-(1/\pi)(1+\alpha^2)$.

A very important application of Eq. (46) can be made to impurities for which $Z=0$, an example of which is Fe dissolved in Ru. In this case, $V=0$, and the condition is simply $\eta(E_f)J > 1$ for magnetization. This condition remains true even if several bands are involved. Suppose that a fraction x of the density of states is contributed by the dominant band and a fraction $(1-x)$ by all other bands. Then it is clear from Eq. (32) that the condition becomes $x\eta(E_f)J/[1-J(1-x)\eta(E_f)] > 1$ or $\eta(E_f)J > 1$.

Now, Fe in Ru is not magnetic, and we know that $\eta(E_f) = 0.44$ states/atom/eV,¹³ so that $J < 2.3$ eV, in

¹³ R. H. Batt and N. E. Phillips quoted in T. H. Geballe, Rev. Mod. Phys. **36**, 134 (1964).

this case. Similarly, Co in Rh is not magnetic.¹⁴ Since $\eta(E_f)$ for Rh is 1.0 states/eV/atom, we conclude that J for Co is less than 1 eV. Ni is magnetic in Pd but is nonmagnetic in Pt.¹⁴ We have $\eta(E_f)$ for Pd and Pt equal to 1.97 and 1.36 states/eV/atom, respectively. Hence for nickel, $0.51 \text{ eV} < J < 0.74 \text{ eV}$.

c. Knight Shift

Considering a single band of electrons, the Knight shift of an impurity atom can be written¹⁵

$$k = (8\pi/3)\chi V |\Psi_{E_f}(0)|^2, \quad (47)$$

where χ is the susceptibility per unit volume of the crystal and is not affected by a single impurity. We approximate $\Psi_{E_f}(0)$ by its component in the central Wannier function so that

$$k = \frac{8\pi}{3}\chi\Omega |W(0)|^2 \left| \frac{1}{1+VG_E(0)} \right|_{E_f}^2 \quad (48)$$

$$= \frac{8\pi}{3}\chi\Omega |W(0)|^2 \times \left\{ \frac{1}{[\alpha(\pi\eta(E_f)V) - 1]^2 + (\pi\eta(E_f)V)^2} \right\}. \quad (49)$$

Then the Knight shift can be written

$$k = \frac{8\pi}{3}\chi\Omega |W(0)|^2 \left[-\pi \frac{dN}{d(\pi\eta(E_f)V)} \right]. \quad (50)$$

Let us set $|W(0)|^2 = |\Phi(0)|^2\xi$, where $\Phi(0)$ is the wave function of a valence electron of the impurity atom, and ξ is a correction factor for a given solvent. We have, then,

$$k = \frac{8\pi}{3}\chi\Omega |\Phi(0)|^2\xi \left[-\pi \frac{dN}{d(\pi\eta(E_f)V)} \right]. \quad (51)$$

In the usual discussion of Knight shift in alloys, the factor in square brackets is ignored. Referring to Fig. 2, for example, this factor is just $-\pi$ times the slope of the curve at the point A for a given self-consistent potential, and can vary over a wide range. In particular, for large $|Z|$, the stable intersections are at large positive or negative values of the abscissa, where the slope is small and the Knight shift should be greatly reduced. An example of this effect may be offered by the case of vanadium dissolved in palladium,¹⁶ where it is observed that the Knight shift of the V nucleus does not reflect the temperature-dependent susceptibility of the Pd solvent.

¹⁴ R. M. Bozorth, D. D. Davis, and J. H. Wernick, J. Phys. Soc. Japan **17**, 112 (1962).

¹⁵ C. H. Townes, C. Herring, and W. D. Knight, Phys. Rev. **77**, 852 (1950).

¹⁶ V. Jaccarino, J. A. Seitchik, and J. H. Wernick (private communication).

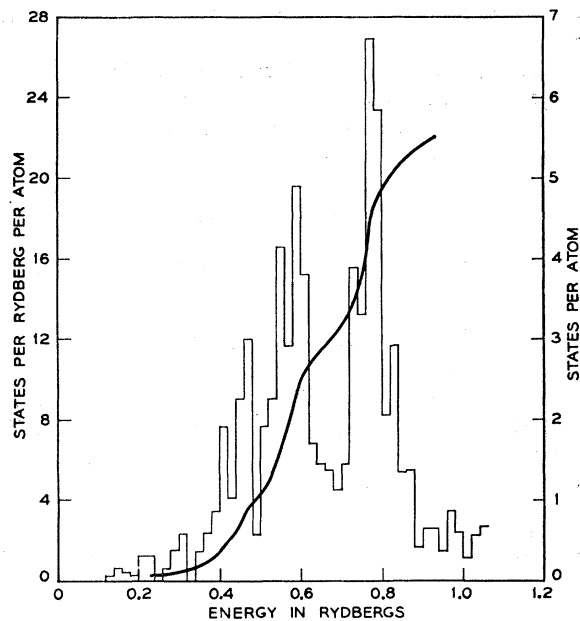


FIG. 6. Density of states and integrated state density as a function of energy for nonmagnetic bcc iron as calculated by J. H. Wood.

d. Fe in the bcc Second-Row Transition Metals

As an approach to a semiquantitative application of the ideas considered in previous sections, we now discuss in more detail the case of iron as a very dilute impurity in the body-centered-cubic $4d$ transition metals. When dissolved in these metals, iron sometimes exhibits a magnetic moment and sometimes does not. The magnetic moment as observed by a measurement of paramagnetic susceptibility is a smooth function of electron concentration, as shown in Fig. 5 adapted from Ref. 6. Proceeding in the direction of increasing electron concentration, a magnetic moment first appears at $\text{Nb}_{0.6}\text{Mo}_{0.4}$ and rises to $2.1 \mu_B$ at Mo. The bcc phase is maintained to $\text{Mo}_{0.6}\text{Re}_{0.4}$. Beyond this point the hexagonal phase sets in and the moment decreases, becoming zero in Tc and Re and remaining zero through Ru. The dotted line represents measurements taken with alloys of Mo and Rh.

The band structure of nonmagnetic bcc Fe has been calculated by Wood,¹⁷ using the augmented plane-wave method. His density-of-states curve is reproduced in Fig. 6, along with the integrated curve giving the number of states below energy E . The double-peaked shape of the band is characteristic of the body-centered-cubic metals. The upper part of the band contains approximately two states per atom and is derived largely from the d states of e_g symmetry.

We adapt this band structure to our use as follows. First, the upper part of the band is represented by two superimposed Lorentzian bands of width $\Delta=0.0254$ Ry

centered at 0.76 Ry and having a peak density of states equal to 12.5 states/Ry. These superimposed bands are shown in Fig. 7, together with a smoothed curve representing the remaining state density in Fig. 6. This remaining state density is derived largely from states of t_{2g} symmetry lying below 0.7 Ry and from an s -like band contributing roughly 1.5 to 2 states/Ry-atom. For iron there are 8 electrons per atom. The Fermi level then lies at the point where the integrated-state density curve crosses 4 states/atom, or at 0.76 Ry, where we have located the center of the Lorentzian bands.

Secondly, the band structure of iron must be adapted to the $4d$ series of metals. Following recent work of Mattheiss,¹⁸ we do this by increasing the energy scale by a factor of 1.48 and decreasing all state densities by a factor of 0.676. For a body-centered-cubic form of Ru (so far unknown), the Fermi level would lie at the peak of the expanded Lorentzian bands in this model of the band structure. Suppose now we make the rigid-band assumption. As Tc(Re) is alloyed into Ru, the Fermi energy decreases. It further decreases in the alloys of Mo and Tc(Re), and for alloys of Nb and Mo. A minimum is found in experimental measurements¹⁹ of specific heat for these alloys near Mo, corresponding to the minimum in state density for 6 electrons at 0.68 Ry, shown in Fig. 6.

We now measure energies δE_f from the peak of the Lorentzian bands. If in a given alloy the Fermi level is a distance δE_f from the peak, we have, from Eq. (39), $\alpha = \delta E_f / \Delta$. In this alloy, iron then appears as an impurity with a valence difference δZ which is twice the number of states per atom through which the Fermi

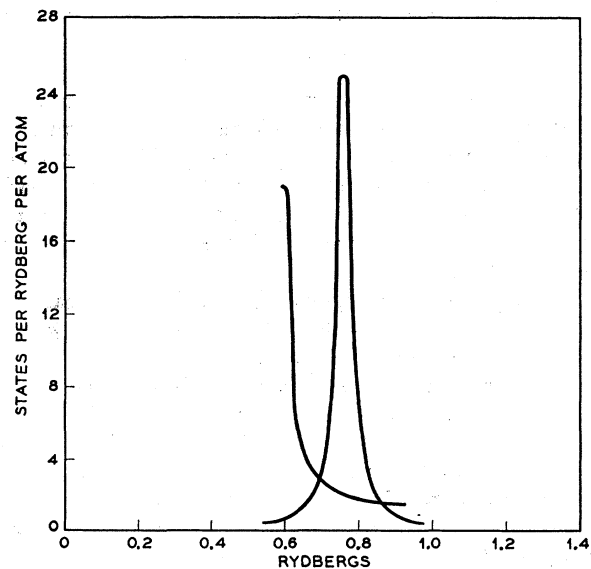


FIG. 7. Smoothed density of states for upper and lower parts of the band for bcc nonmagnetic iron adopted from Fig. 6.

¹⁷ J. H. Wood, Phys. Rev. **126**, 517 (1962).

¹⁸ L. F. Mattheiss (private communication).

¹⁹ F. J. Morin and J. P. Maita, Phys. Rev. **129**, 1115 (1963).

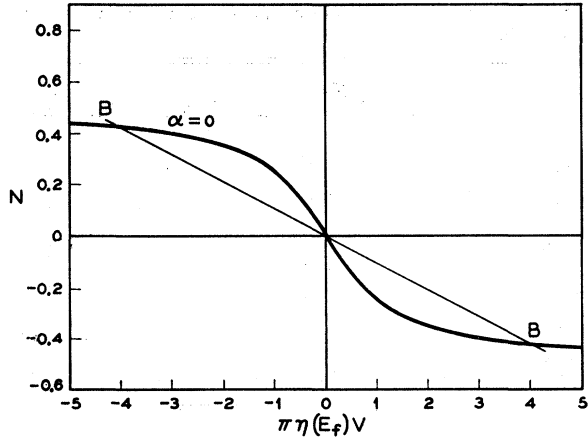


FIG. 8. Solution of the self-consistent potential for Fe in bcc Ru. $F=30$, $U=20$, $J=2$, $\delta Z=0$, $\alpha=0$. Stable magnetic solutions are at B.

level has dropped proceeding from Ru. Using Fig. 6, one can then construct Table I, which gives, for various values of α , δE_f in electron volts, δZ , the density of states $\eta(E_f)$ for each Lorentzian band in states/eV-atom, and the total smoothed density of states $\xi(E_f)$ for all bands.

In the calculation which follows, we assume that the two superimposed Lorentzian bands (bands 1 and 2) behave exactly alike so that $N_\sigma = N_{1\sigma} = N_{2\sigma}$. We also assume that these two bands dominate the self-consistent shielding of the impurity atom. Proceeding as in Sec. IIe, we find

$$\frac{1}{2}(N_\uparrow + N_\downarrow) = \frac{F\delta Z}{2(2U-J)} + \frac{1+\beta(2U-J)}{2(2U-J)\pi\eta(E_f)} \times \pi\eta(E_f)\frac{1}{2}(V_\uparrow + V_\downarrow), \quad (52)$$

$$(N_\uparrow - N_\downarrow) = -\frac{1-\beta J}{2J\pi\eta(E_f)} \pi\eta(E_f)(V_\uparrow - V_\downarrow), \quad (53)$$

$$\sum_l N_{l\sigma} = -\beta V_\sigma, \quad (54)$$

TABLE I. Parameters used in impurity calculation for Fe in the 4d transition-metal alloys.

α	δE_f eV	δZ	$\eta(E_f)$ states/eV- atom	$\xi(E_f)$ states/eV- atom
0	0.00	0.00	0.622	1.34
$-\frac{1}{4}$	-0.13	0.30	0.585	1.34
$-\frac{1}{2}$	-0.26	0.50	0.497	1.10
$-\frac{3}{4}$	-0.38	0.65	0.398	0.90
-1	-0.51	0.80	0.311	0.73
$-\frac{3}{2}$	-0.77	1.25	0.191	0.50
-2	-1.02	1.65	0.124	0.38
-3	-1.53	1.95	0.062	0.28
-4	-2.04	2.15	0.036	0.27
-5	-2.55	2.45	0.024	0.34
-6	-3.07	2.85	0.016	0.76

TABLE II. Constants used in finding self-consistent potential for Fe impurity in 4d transition-metal alloys. $F=30$ eV, $U=20$ eV, $J=2$ eV, $\beta=0.1$ states/eV-atom.

α	$F\delta Z/2(2U-J)$	$1+\beta(2U-J)$	$1-\beta J$
		$2(2U-J)\pi\eta(E_f)$	$2J\pi\eta(E_f)$
0	0.000	0.0323	0.102
$-\frac{1}{4}$	0.118	0.0344	0.109
$-\frac{1}{2}$	0.197	0.0405	0.128
$-\frac{3}{4}$	0.257	0.0505	0.160
-1	0.316	0.0646	0.205
$-\frac{3}{2}$	0.493	0.1052	0.334
-2	0.652	0.1620	0.514
-3	0.769	0.324	1.025
-4	0.848	0.552	1.740
-5	0.967	0.845	2.67
-6	1.125	1.200	3.79

where the sum on l is over all active bands except bands 1 and 2 and $\beta = \sum_l \eta_l(E_f)$ as before. In the present case, we suppose that the 4d subbands in the lower part of the band are so nearly filled in all cases that they contribute very little to the shielding of the impurity. We take β , therefore, equal to the s -band state density, which is approximately 0.1 state/eV-atom. As before we take $F=30$ eV, $U=20$ eV, and $J=2$ eV. The constants appearing in Eqs. (52) and (53) for various values of α can then be calculated and are listed in Table II.

The solution of the self-consistent problem presented by Eqs. (52) and (53) can be found graphically, as is done in Sec. IIIb. Examples of these graphical solutions for $\alpha=0$, -1 , -3 are shown in Figs. 8, 9, and 10. The values of N_σ and V_σ found in this way are listed in Table III. From equation (54) we can obtain $\sum_l N_{l\sigma}$, and this is also listed in Table III. Finally, we are interested in the polarization induced on the nearest neighbors to the impurity. This can be obtained from Eqs. (20) and (24), where we assume that a reasonable

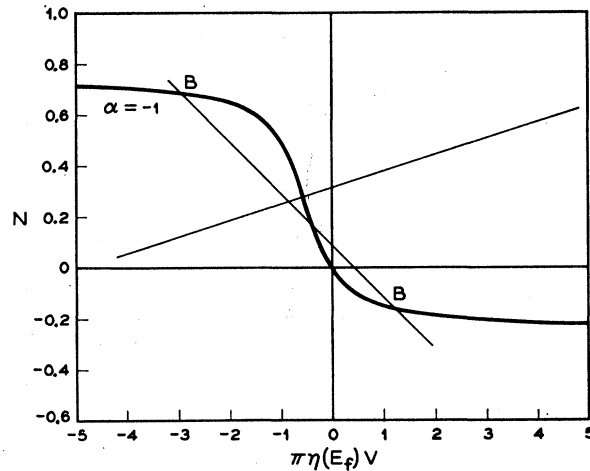


FIG. 9. Solution of the self-consistent potential for Fe in bcc $Tc_{0.8}Ru_{0.2}$. $\delta Z=0.8$, $\alpha=-1$, other parameters as in Fig. 8. Stable magnetic solutions are at B.

TABLE III. Polarization in Bohr magnetons of the central impurity atom and of the nearest-neighbor atoms as calculated for Fe dissolved in various 4d metal alloys. $j=0.2$ eV.

α	$N_{1\uparrow}$	$N_{1\downarrow}$	$\pi\eta(E_f)V_{\uparrow}$	$\pi\eta(E_f)V_{\downarrow}$	$2(N_{1\uparrow}-N_{1\downarrow})$	$\sum_i N_{i\uparrow}$	$\sum_i N_{i\downarrow}$	$\sum_i (N_{i\uparrow}-N_{i\downarrow})$	$\frac{2(N_{\uparrow}-N_{\downarrow})}{\sum_i (N_{i\uparrow}-N_{i\downarrow})}$	$8 \sum_m (N_{m\uparrow'}-N_{m\downarrow'})$	Total moment
0	0.42	-0.42	-4.03	4.03	1.68	0.21	-0.21	0.42	2.10	4.50	6.66
-1/4	0.51	-0.34	-4.75	3.15	1.70	0.26	-0.17	0.43	2.13	4.57	6.70
-1/2	0.58	-0.26	-4.23	2.35	1.68	0.27	-0.15	0.42	2.10	3.70	5.80
-3/4	0.64	-0.21	-3.55	1.77	1.70	0.28	-0.14	0.42	2.12	3.05	5.17
-1	0.69	-0.16	-2.92	1.24	1.70	0.30	-0.13	0.43	2.13	2.49	4.62
-5/4	0.76	0.00	-2.32	0.00	1.52	0.38	0.00	0.38	1.90	1.52	2.42
-2	0.79	0.26	-1.37	-0.34	1.06	0.35	0.09	0.26	1.32	0.80	2.12
-3	0.83	0.37	-0.74	-0.30	0.92	0.38	0.15	0.23	1.15	0.52	1.67
-4	0.84	0.48	-0.46	-0.25	0.72	0.40	0.22	0.18	0.90	0.39	1.29
-5	0.85	0.60	-0.33	-0.20	0.50	0.44	0.27	0.17	0.67	0.36	1.03
-6	0.85	0.85	-0.25	-0.25	0.00	0.47	0.47	0.00	0.00	0.00	0.00

value for j is 0.2 eV and take $J'=0$. For the neighbors we take $\xi(E_f)$ to be the total density of states, since the potentials are so small at the near-neighbor sites that all bands contribute. The total polarization contributed by the 8 near neighbors is listed in Table III as $8 \sum_m (N_{m\uparrow'} - N_{m\downarrow'})$. Table III shows, finally, the total moment associated with the impurity complex.

The principal results of the calculation are shown in Fig. 11, which gives the moment on the impurity atom and the total moment of the complex as a function of the valence difference of the impurity. These results may be compared with the experimental facts shown in Fig. 5. Considering the many uncertainties of the theoretical model, the agreement is quite satisfactory. To the left of the bcc-hcp boundary, where the comparison can be made, the model predicts a total moment of about $2 \mu_B$, as is observed. As δZ increases, the moment decreases and goes to zero at about the same alloy composition as found experimentally. The model does, however, predict a less precipitous decrease of the moment in the alloys near Mo than is found for the

measured moments. The slope of the curve in this region is rather sensitive to the choice of parameters and could be made to resemble the experimental curve more closely by a somewhat different choice of the exchange constant J and the s -band density of states β . One of the most important conclusions to be drawn from the calculation is that a reasonable description of the experimental results can be made using an exchange constant no larger than 2 eV. It is clearly not necessary to have J as large as 10–20 eV in order to maintain a magnetic moment in these alloys.

It is interesting to note the rather substantial difference that exists between the moment that resides on the central impurity atom alone and the total moment of the complex of impurity atom and its near neighbors. In the case of molybdenum ($\delta Z=2$), these moments are approximately $1.5 \mu_B$ and $1.1 \mu_B$ in our calculation. Experimentally, the total moment is observed to be $2.1 \mu_B$ ⁶ and the density of states to be¹⁹ 0.42 state/eV-atom. (This value is probably enhanced by electron-

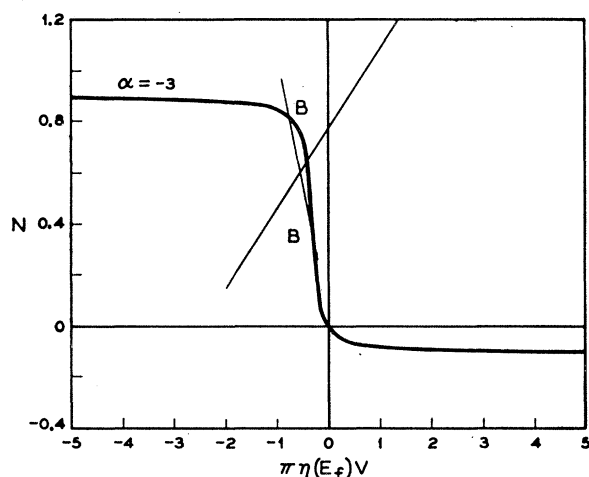


FIG. 10. Solution of the self-consistent potential for Fe in bcc $\text{Mo}_{0.95}\text{Tc}_{0.05}$. $\delta Z=1.95$, $\alpha=-3$, other parameters as in Fig. 8. Stable magnetic solutions are at B.

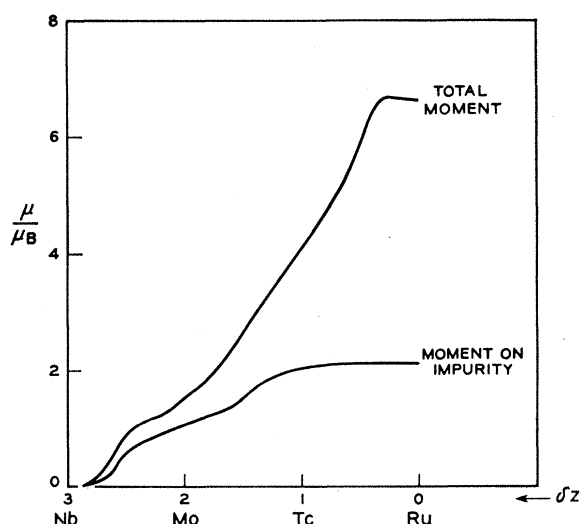


FIG. 11. Calculated magnetic moment as a function of valence difference for iron dissolved in various bcc 4d transition metal alloys.

phonon interactions.) The moment resident on the central atom would then be $1.2 \mu_B$, assuming once more that $j=0.2$ eV. This discrepancy between the impurity moment and the total moment may account, in part, for the results of Mössbauer-effect measurements made on Fe dissolved in Mo which show an unexpectedly small hyperfine field at the nucleus of the iron atom.²⁰

In carrying out this calculation, one very important feature has emerged. That is the rather profound effect produced upon the self-consistent problem by the shielding due to the s -band density of states. If β is taken equal to zero in Eqs. (52) and (53), no self-consistent magnetic moment can be maintained beyond about $\delta Z=2$, and agreement with experiment would be rather poor.

Finally, we should like to remark on the results obtained to the right of the bcc-hcp boundary which relate to a group of hypothetical bcc alloys. If these alloys could be experimentally obtained in bcc form, the theory predicts that iron would exhibit a magnetic moment in dilute solution all the way to Ru or $\delta Z=0$. Furthermore, it is predicted that the total magnetic moment would become large in these alloys, approaching

²⁰ P. P. Craig, D. E. Nagle, W. A. Stegert, and R. D. Taylor, Phys. Rev. Letters **9**, 12 (1962).

$6.5 \mu_B$ near Ru. This occurrence of giant moments is a familiar effect observed in alloys near palladium.⁶

Note added in proof. In connection with the discussion in Sec. IIIb, it is worth noting that the Stoner criterion for the instability of the Fermi ground state against separation into two spin bands is also $\eta(E_f)J > 1$. Thus, since Fe is a magnetic metal, following the discussion in Sec. IIIb it must also be possible to find Hartree-Fock states where a single atom is magnetic, although such a state would have a higher energy than the completely magnetic state. It would seem reasonable to suppose that such local magnetic states could be used to describe approximately the condition of iron above its Curie temperature of 1043°K. With an exchange energy of 1 eV and a moment per atom of about 2 Bohr magnetons, the local magnetic moments should be stable to temperatures much higher than the Curie temperature.

ACKNOWLEDGMENTS

We would like to acknowledge stimulating and instructive conversations during the course of this work with P. W. Anderson, M. Lax, V. Jaccarino, L. R. Walker, N. R. Werthamer, L. F. Mattheiss, and J. C. Phillips.